Journal of Biomedical Optics

BiomedicalOptics.SPIEDigitalLibrary.org

Quantitative optical coherence tomography imaging of intermediate flow defect phenotypes in ciliary physiology and pathophysiology

Brendan K. Huang
Ute A. Gamm
Stephan Jonas
Mustafa K. Khokha
Michael A. Choma

SPIE.

Quantitative optical coherence tomography imaging of intermediate flow defect phenotypes in ciliary physiology and pathophysiology

Brendan K. Huang,[a,*] Ute A. Gamm,[b] Stephan Jonas,[b] Mustafa K. Khokha,[c,d] and Michael A. Choma[a,b,c,e]
[a]Yale University, Department of Biomedical Engineering, 55 Prospect Street, New Haven, Connecticut 06511, United States
[b]Yale School of Medicine, Department of Diagnostic Radiology, P.O. Box 208043, New Haven, Connecticut 06520, United States
[c]Yale School of Medicine, Department of Pediatrics, P.O. Box 208064, New Haven, Connecticut 06520, United States
[d]Yale School of Medicine, Department of Genetics, 333 Cedar Street, New Haven, Connecticut 06510, United States
[e]Yale University, Department of Applied Physics, P.O. Box 208267, New Haven, Connecticut 06520, United States

Abstract. Cilia-driven fluid flow is a critical yet poorly understood aspect of pulmonary physiology. Here, we demonstrate that optical coherence tomography-based particle tracking velocimetry can be used to quantify subtle variability in cilia-driven flow performance in *Xenopus*, an important animal model of ciliary biology. Changes in flow performance were quantified in the setting of normal development, as well as in response to three types of perturbations: mechanical (increased fluid viscosity), pharmacological (disrupted serotonin signaling), and genetic (diminished ciliary motor protein expression). Of note, we demonstrate decreased flow secondary to gene knockdown of *kif3a*, a protein involved in ciliogenesis, as well as a dose-response decrease in flow secondary to knockdown of *dnah9*, an important ciliary motor protein. [DOI: 10.1117/1.JBO.20.3.030502]

Keywords: mucus; *Xenopus*; optics; particle tracking; *dnah9*; *kif3a*.

Paper 140826LR received Dec. 12, 2014; accepted for publication Feb. 19, 2015; published online Mar. 9, 2015.

Cilia-driven fluid flow clears mucus, bacteria, and particulates from the lungs.[1] Despite its importance, it is a poorly understood aspect of respiratory physiology. Severe dysfunction of cilia in conditions such as primary ciliary dyskinesia (PCD) is associated with impaired respiratory mucus clearance and recurrent pulmonary infections. It is unknown, however, if subtle variations in cilia-driven mucus clearance underlie clinically significant changes in respiratory diseases severity, such as in asthma.

Prior measurements of ciliary flow have shown that flow speed can vary considerably between different specimens within an experimental population.[2,3] Additionally, within a single specimen, flow has been previously described to vary as a function of distance from the cilia.[4,5] Thus, when quantifying subtle variations in ciliary performance, it can be helpful to make cross-sectional measurements localized near a ciliated surface. Given these considerations, there has been increasing interest in applying optical coherence tomography (OCT), a modality that offers both ~1- to 10-μm scale resolution and depth-resolved, cross-sectional imaging, toward studying ciliary physiology.[5–7]

We previously demonstrated that OCT-based particle tracking velocimetry (OCT-PTV) could be used to estimate the velocity flow field in the *Xenopus* animal model system.[5] In this letter, we build on these results and show that OCT-PTV can be used to quantify subtle changes induced by physical, chemical, and genetic perturbations. We quantify changes in ciliary flow due to changes in the viscosity of the fluidic environment, disruption of the serotonin signaling pathway, and diminished molecular expression of two important ciliary proteins, *dnah9* and *kif3a*. Additionally, we use OCT-PTV to characterize the developmental process of a ciliated surface.

Xenopus embryos (tadpoles), including *X. laevis* and *X. tropicalis* species, express cilia on their epithelial surface during development. The cilia themselves provide a time-varying backscattered signal that can be detected by OCT. Using speckle variance processing, we identified ciliated patches of the epithelium [Fig. 1(a) and Video 1], consistent with the methods described in Ref. 6. The ciliated patches in turn drive a microfluidic flow that can also be imaged using OCT. After immobilizing the embryo with benzocaine and seeding 10 μm microspheres in the fluid, we used OCT-PTV to estimate the microfluidic vector flow field, a spatial map showing the direction and magnitude of flow velocity at each location relative to a ciliated surface [Fig. 1(b)]. Of note, although chemical anesthetics have the potential to alter flow, benzocaine was previously described to have no discernable effect on ciliary performance,[8] and we observed no visible effects.

Flow field estimation using OCT-PTV provides a two-dimensional (x, y), two-component (v_x, v_y) description of steady-state flow. Flow near the surface of the embryos is consistently directed head to tail, but flow more than several hundreds of microns from the surface varied in magnitude and directionality depending on the exact positioning of the embryo in the well. As such, we extracted only the component of flow spatially near the surface and directed along it a metric we denote as the average tangential flow speed. The tangential flow speed was calculated by manually drawing a line tangent to the surface of the embryo, extracting the flow field measurements <100 μm above the line and projecting each velocity vector along the tangent vector. These tangential flow measurements over the length of the embryos were then averaged to give the average tangential flow speed.

In order to verify that average tangential flow speed could be used to quantify changes in ciliary flow, we first tested the effects of a simple physical perturbation, an increase in viscosity. We increased the viscosity of the physiologic solution [1/9× modified Ringer's (MR) solution] surrounding *X. tropicalis* embryos by adding high molecular weight dextrans (Sigma 95771, MW 2,000,000) to final concentrations of 1.3% and

*Address all correspondence to: Brendan K. Huang, E-mail: brendan.huang@yale.edu

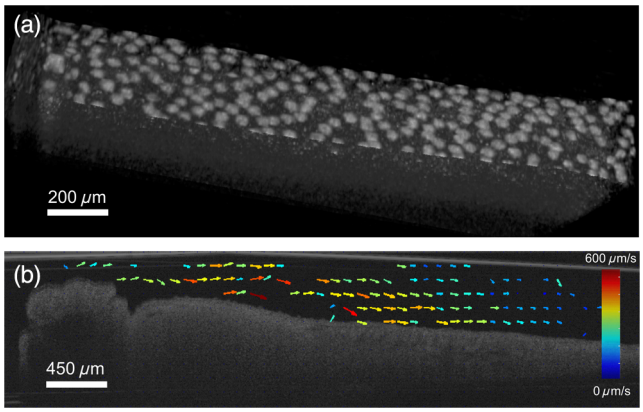

Fig. 1 (a) Optical coherence tomography (OCT) speckle variance identifies ciliated epithelial cells (Video 1, MOV, 1.05 MB) [URL: http://dx.doi.org/10.1117/1.JBO.20.3.030502.1]. (b) Flow field generated by OCT-based particle tracking velocimetry.

2.3%. These concentrations lead to an expected viscosity of 2.0 and 2.95 cP (2× and 3×) as estimated from Ref. 9. As the viscosity of the solution surrounding each embryo was doubled and tripled [Fig. 2(a)], the relative tangential flow speed was decreased by an average factor of $2.1 \pm 0.2\times$ and $3.0 \pm 0.3\times$ (standard error of mean), respectively. Thus, we were able to quantify changes in ciliary flow speed due to a simple physical perturbation.

We next investigated the effects of pharmacological intervention on ciliary flow. It has been shown in *Xenopus* embryos that depletion of serotonin, an important signaling molecule, can decrease flow rates while repletion can restore flow.[3] Following the pharmacological protocol in Ref. 3, we incubated *X. tropicalis* embryos with (1) control 1/9× MR, (2) 150 μM para-chlorophenylalanine (PCPA) (4-chloro-DL-phenylalanine methyl ester hydrochloride), an agent which depletes endogenous serotonin stores, and (3) 150 μM PCPA plus 1 mM serotonin hydrochloride for repletion. Indeed, we observed that decreased flow in the PCPA-only group was rescued by the addition of serotonin [Fig. 2(b)].

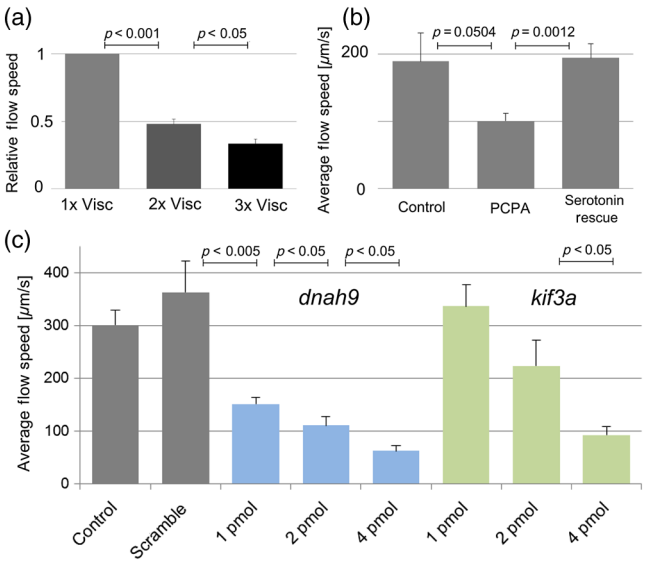

Fig. 2 Quantification of physical, chemical, and biological perturbations of ciliary function in (a and b) *X. tropicalis* and (c) *X. laevis*. All error bars showing standard error of mean (SEM). (a) Effects of increased viscosity on average tangential flow speed ($n = 13$), with relative viscosity of 1× equal to that of water. (b) Rescue of diminished ciliary flow from PCPA using serotonin ($n = 15$). (c) Dose-dependent knockdown of *dnah9* ciliary motor protein ($n = 15$–18) leads to intermediate defects in flow while knockdown of *kif3a* (1 pmol $n = 11$, 2 pmol $n = 10$, 4 pmol $n = 6$) only leads to statistically significant decrease at highest dose.

We next sought to characterize novel genetic-based phenotypes. PCD can be caused by disruption in a number of genes including dynein and kinesin motor proteins.[10] Common to all these genetic abnormalities is that ciliary dysfunction is defined by complete disruption of the gene, an all-or-nothing phenotype. Another plausible mechanism of disease, however, is the decreased expression of the same genes. Thus, we investigated the effects of intermediate, but not complete, knockdown of dynein axonemal heavy chain 9, *dnah9*, a dynein motor protein responsible for generation of movement and force in cilia, as well as kinesin family member 3a, *kif3a*, a kinesin motor protein involved in ciliogenesis.

In order to assess the effects of intermediate levels of ciliary gene expression on the flow phenotype, we used morpholino oligonucleotides, a type of antisense technology that can decrease protein expression by preventing mRNA splicing or translation.[11] Due to the existence of previously characterized morpholinos in *X. laevis*, we chose to investigate knockdown in *X. laevis*, a comparable system to *X. tropicalis* with a higher baseline flow speed. Using the *dnah9* splice-blocking morpholino as previously described in Ref. 8, we injected varying doses into single-cell zygotes, ranging from 1 to 4 picomoles (pmol) per embryo. We coinjected an Alexa488 (Invitrogen) tracer into the embryos to verify proper delivery after 24 h. As shown in Fig. 2(c), increased morpholino dosing diminished average tangential speed in a dose-dependent manner when compared with both the uninjected controls, as well as a negative control injected with 4 pmol of a scramble morpholino sequence. Thus, we observed intermediate decreases in ciliary flow due to intermediate decreases in gene expression. This result highlights how subtle variations in ciliary function can be modulated by plausible molecular mechanisms, and how quantitative imaging can enable the detection of these intermediate phenotypes.

We also investigated the effects of disrupting the kinesin motor protein *kif3a* [Fig. 2(c)]. Under-expression of *kif3a* has been associated with a more severe asthma phenotype.[12] Using sequence information available on Xenbase,[13] we designed a morpholino to bind to the first splice site of *kif3a* in *X. laevis* (sequence 5′-AGAGCCTCTCCTTACCGGCATTGTT-3′). Noting that an 8 pmol dosage leads to nonspecific embryo toxicity, we injected single-cell zygotes with 1 to 4 pmol. We found that, in contrast to *dnah9*, there was not a significant difference between the 1 and 2 pmol groups of *kif3a* (the power of comparison was 0.81). Only the highest dose of 4 pmol leads to a statistically significant decrease in flow ($p = 0.03$ for 2 to 4 pmol comparison, as calculated by the Mann–Whitney U test). Indeed, not all genes would necessarily be expected to generate intermediate phenotypes, but some may lead to binary phenotypes after knockdown past a given threshold. More studies increasing the number of dosing levels as well as quantifying protein expression would further elucidate this hypothesis.

Lastly, we used OCT to investigate how a ciliated surface transitions from the absence of flow to the presence of flow. Like other organs, ciliated surfaces undergo a developmental process. The development of coordinated ciliary flow in

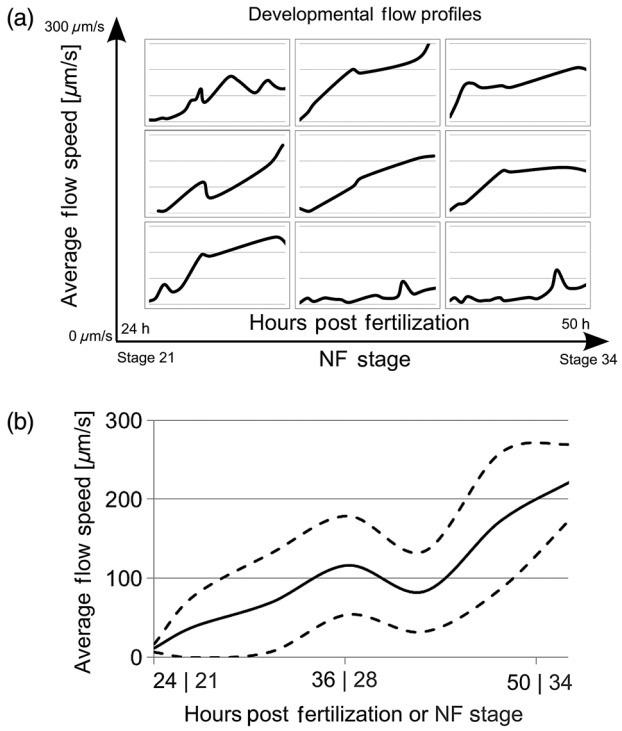

Fig. 3 (a) Longitudinal measurements of developmental flow on nine different embryos (Video 2, MOV, 312 KB) [URL: http://dx.doi.org/10.1117/1.JBO.20.3.030502.2] and (b) aggregate data showing mean ± standard deviation during 24 to 50 h postfertilization, or approximately Nieuwkoop–Faber (NF) stages 21 to 34.

Xenopus embryos is known to occur over approximately 24 h and to involve the interplay between tissue patterning and hydrodynamic signaling.[14] In spite of having been extensively studied from a molecular perspective, however, to our knowledge, the flow speed during this period has not yet been described in a longitudinal and quantitative manner. Thus, we quantified the average tangential speed during the onset of flow during 24 to 50 h, corresponding approximately to Nieuwkoop–Faber (NF) developmental stages 21 to 34 in *X. laevis*.[15] We imaged nine embryos over this period, with measurements taken every 2 to 4 h [Fig. 3(a), Video 2]. For each measurement, the embryo was immobilized with benzocaine and suctioning for the duration of imaging (~5 min), and then immediately washed and placed in a reservoir of clean 1/3× MR. Aggregating the data, we generated a normative curve [Fig. 3(b)] showing the average flow plus or minus one standard deviation (STD). Embryos began the process with an average flow speed of $11 \pm 5\ \mu\mathrm{m/s}$ (STD) at NF stage 21, and increased to $232 \pm 49\ \mu\mathrm{m/s}$ by approximately stage 34. Notably, 2/9 embryos failed to develop a sustained flow $>100\ \mu\mathrm{m/s}$ during this period.

In conclusion, the physiology of cilia-driven fluid flow is important for respiratory disease, but it is currently unknown whether small perturbations can cause intermediate defects in ciliary flow. Here, we have used OCT to show that genetic perturbations can cause intermediate flow phenotypes. We were also able to characterize flow in a developmental context. OCT-PTV is well-suited toward quantifying subtle changes because it can be used to interrogate flow near a ciliated surface with high spatial resolution. Based on our results, we believe that OCT-PTV will continue to find an important role in quantitatively investigating microfluidic ciliary physiology.

Acknowledgments

This work was supported by March of Dimes Basil O'Connor Starter Scholar Research Award and NIH1R01HL118419-01. B.K.H. was additionally supported by NIH MSTP TG T32GM07205. M.K.K. was supported by 1R21HL120783 and 1R01HD081379.

References

1. B. Huang and M. Choma, "Microscale imaging of cilia-driven fluid flow," *Cell. Mol. Life Sci.* **72**(6), 1095–1113 (2015).
2. L. N. Vandenberg, J. M. Lemire, and M. Levin, "Serotonin has early, cilia-independent roles in *Xenopus* left-right patterning," *Dis. Model Mech.* **6**(1), 261–268 (2012).
3. P. Walentek et al., "A novel serotonin-secreting cell type regulates ciliary motility in the mucociliary epidermis of *Xenopus* tadpoles," *Development* **141**(7), 1526–1533 (2014).
4. W. Supatto, S. E. Fraser, and J. Vermot, "An all-optical approach for probing microscopic flows in living embryos," *Biophys. J.* **95**(4), L29–L31 (2008).
5. S. Jonas et al., "Microfluidic characterization of cilia-driven fluid flow using optical coherence tomography-based particle tracking velocimetry," *Biomed. Opt. Express* **2**(7), 2022–2034 (2011).
6. A. L. Oldenburg et al., "Monitoring airway mucus flow and ciliary activity with optical coherence tomography," *Biomed. Opt. Express* **3**(9), 1978–1992 (2012).
7. L. B. Liu et al., "Method for quantitative study of airway functional microanatomy using micro-optical coherence tomography," *PLoS One* **8**(1), e54473 (2013).
8. P. Vick et al., "Flow on the right side of the gastrocoel roof plate is dispensable for symmetry breakage in the frog *Xenopus laevis*," *Dev. Biol.* **331**(2), 281–291 (2009).
9. L. Gheber, A. Korngreen, and Z. Priel, "Effect of viscosity on metachrony in mucus propelling cilia," *Cell Motil. Cytoskeleton* **39**(1), 9–20 (1998).
10. M. Fliegauf, T. Benzing, and H. Omran, "When cilia go bad: cilia defects and ciliopathies," *Nat. Rev. Mol. Cell Biol.* **8**(11), 880–893 (2007).
11. M. K. Khokha et al., "Techniques and probes for the study of *Xenopus* tropicalis development," *Dev. Dyn.* **225**(4), 499–510 (2002).
12. M. B. Kovacic et al., "Identification of KIF3A as a novel candidate gene for childhood asthma using RNA expression and population allelic frequencies differences," *PLoS One* **6**(8), e23714 (2011).
13. J. B. Bowes et al., "Xenbase: a *Xenopus* biology and genomics resource," *Nucleic Acids Res.* **36**(Database issue), D761–D767 (2007).
14. B. Mitchell et al., "The PCP pathway instructs the planar orientation of ciliated cells in the *Xenopus* larval skin," *Curr. Biol.* **19**(11), 924–929 (2009).
15. P. D. Nieuwkoop and J. Faber, *Normal Table of Xenopus laevis (Daudin): A Systematical and Chronological Survey of the Development From the Fertilized Egg Till the End of Metamorphosis*, Garland Pub., New York (1994).